Laser Raman studies on compounds 7.O4O.7 and 7.O5O.7

B. Gogoi[a]; A. Bhattacharjee[b]; P. R. Alapati[a]; A. L. Verma[ac]

[a] Department of Physics NERIST Nirjuli 791 109 India, [b] Department of Physics NEHU Shillong 793 022 India, [c] Director NERIST Nirjuli 791 109 India,

PLEASE SCROLL DOWN FOR ARTICLE

Laser Raman studies on compounds 7.O4O.7 and 7.O5O.7

B. GOGOI, A. BHATTACHARJEE†, P. R. ALAPATI and A. L. VERMA†‡*

Department of Physics, NERIST, Nirjuli 791 109, India
†Department of Physics, NEHU, Shillong 793 022, India
‡Director, NERIST, Nirjuli 791 109, India

Laser Raman studies on two compounds of the α,ω-bis(4-alkylanilinebenzylidene -4′-oxy)alkane series were carried out in the spectral regions 1140–1220 and 1550–1650 cm^{-1} as a function of temperature. Compounds 7.O4O.7 and 7.O5O.7, exhibit SmA and SmF phases. The structural differences between these liquid crystal dimers, having either an odd or an even number of carbon atoms in the spacer, are remarkably existent in the room temperature Raman spectra. The results are rationalized on the basis of the tendency of these compounds to exhibit bent shapes, and how this manifests in the odd–even effect at the molecular level assuming a semi-rigid core region of the dimeric molecule. It is found that the behaviour of the odd spacer dimer (7.O5O.7) agrees with the molecular model, whereas the even spacer dimer (7.O4O.7) behaves in a similar fashion to monomeric compounds such as the nO.m. compounds. In both cases, dynamic changes around the C=N bond have a profound effect both on the molecular shape in the different phases and on phase behaviour.

1. Introduction

Dimeric liquid crystals are formed by the linking of two mesogenic groups by an alkyl chain (spacer). Liquid crystal dimers have attracted considerable interest in recent years, both theoretically and experimentally, due to their unusual properties as compared with conventional low molar mass liquid crystals. They serve also as model compounds for semi-flexible main chain liquid crystal polymers [1–8]. These dimers are divided into two categories: symmetric dimers and non–symmetric dimers. In the former class, both mesogenic groups are identical, whereas in the latter the two mesogenic groups are different. The nematic–isotropic transition temperatures of these dimeric compounds exhibit a marked alternation as the number of carbon atoms in the alkyl spacer changes from odd to even. However, this alternation decreases as the spacer grows in length. In contrast, the alternation seen for the entropy change associates with the nematic–isotropic transition is essentially unattenuated, at least for spacers containing up to twelve carbon atoms [9]. In addition, the entropy change at the nematic–isotropic transition for dimers having odd spacers is comparable to that of conventional monomers, whilst for compounds containing even spacers, the transition entropy suggests that the orientational order for even members is significantly greater than that for odd members.

Although, detailed studies on dimeric liquid crystals have been conducted using various techniques such as XRD, NMR, ESR and dilatometry [1–12], a thorough investigation to understand the origin of their interesting behaviour at the molecular level has not been reported so far, to the best of our knowledge.

Raman spectroscopy has proved to be a very powerful technique in the investigation of the dynamics of liquid crystalline compounds, because using this technique not only does one obtain information that is bond specific, but also the changes at the microscopic level are observed as measurable quantities [13–15]. The spectra–structure correlations, as well as the connection between structural changes accompanying the phase transition and the corresponding changes in the Raman spectra, are of particular interest. These correlations have been used very effectively to obtain information about liquid crystals at the molecular level, such as details of molecular orientation/rotations, and intra- and inter-molecular interactions.

In the present studies, we have carried out a systematic study using Raman spectroscopy on two liquid crystal dimers belonging to the homologues series, the α-ω-bis(4-alkylanilinebenzylidene -4′-oxy)alkanes (hereafter referred to as m.OnO.m) as a function of temperature. The compounds 7.O4O.7 and 7.O5O.7 were selected for our study as both exhibit the very rare

*Author for correspondence; e-mail: alverma@yahoo.com

SmF–SmA phase transition. In addition, as these compounds differ only by a CH_2 spacer group, we hoped to obtain evidence of the odd–even effect at a molecular level.

Our studies reveal that these dimeric liquid crystalline compounds have very different properties when compared with the monomers. The Raman spectra of these compounds at room temperature show the odd–even effect in a remarkable fashion. From temperature dependent studies, we have explained the very rare SmF–SmA phase transition in terms of orientational/ rotational changes of the various segments of the molecule. We have also attempted to understand the tendencies of these molecule to exhibit bent conformations, and how these are manifested in the odd–even effect at the molecular level.

2. Experimental detail

The compounds were synthesized following a standard procedure as described in the literature [1]. The crude product was recrystallized repeatedly from ethyl acetate until the transition temperatures were found to be constant and reproducible. The differential scanning calorimetric studies were carried out using a Perkin–Elmer DSC7. The various phases exhibited by these compounds were characterized by observing their optical textures under a polarizing microscope equipped with custom built hot stage. The temperature resolution in these microscopic studies was $0.1°C$. The transition temperatures and associated entropy changes were found to be in excellent agreement with literature values [1].

The Raman spectra of the samples were recorded at different temperatures using a Spex Ramalog 1403 double monochromator equipped with a RCA–30134 photomultiplier tube and a CCD detector in the 1140–1220 and 1550–1650 cm^{-1} regions. The spectra were recorded over a wide range of temperature starting from $25°C$ (crystalline phase) to $212°C$ (isotropic phase) for 7.O4O.7 and $145°C$ for 7.O5O.7 at an interval of $0.3°C$ near phase transitions and at $2°C$ intervals elsewhere. For recording the temperature dependent Raman spectra of the samples, two different thermal set-ups were used. In the first, the sample was placed in a small well 2 mm in diameter and 1 mm deep drilled in a square glass slide. This slide was mounted on a FP82 hot stage of a Mettler FP900 system. The temperature stability in this system was maintained to an accuracy of $\pm 0.1°C$. However, this sample was found to be susceptible to laser heating, and thus the experiments were also repeated with the sample confined in a 0.8 mm diameter quartz capillary sealed at both ends and containing an inert atmosphere. This capillary was placed in custom built high temperature glass cell, the
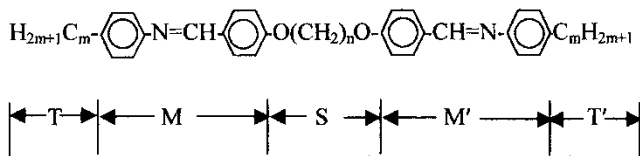
temperature of which could be maintained to an accuracy of $\pm 0.2°C$. A copper–constantan thermocouple was placed in close contact with the sample to monitor the temperature continuously. The excitation source used was a 488.0 nm Ar^+ laser. In order to avoid laser heating of the sample, a very low laser power (20–30 mW) was employed. A scanning increment of $0.3 cm^{-1}$ with an integration time of 1 s were found to be suitable for recording spectra with a reasonably good signal to noise ratio with a slit combination of 200–400–400–200 μm. Our data have very high reproducibility with the uncertainties in peak positions being within $\pm 0.20 cm^{-1}$ for sharp peaks while the band areas and linewidths (FWHM) are accurate to within $\pm 2\%$. The spectra obtained from both temperature control set-ups were found to be highly consistent with respect to each other.

As the spectral parameters (peak positions, linewidths and integrated intensities) were required to be measured precisely, the laser plasma lines were recorded at the same slit setting as used for recording the Raman spectra in order to eliminate slit width effects. A small attachment called 'lasermate' was used to eliminate the spurious plasma lines from the spectra. In order to calculate the slit function, a few spectra were re-recorded without the lasermate. The slit function, $S = 2.62 cm^{-1}$, was calculated as the full width at half maxima (FWHM) of the plasma line recorded at $1576.60 cm^{-1}$ from the Ar^+ laser. In an ideal case, the plasma line should be very close to the position of the Raman band of interest. To approach the bands under study as closely as possible, two more plasma lines at 1138.8 and $1172.5 cm^{-1}$ from the Ar^+ laser were recorded. The FWHM values of these two lines were also found to be $2.62 cm^{-1}$. This value of the slit function was used in fitting the curves and determining their linewidths. The curve fitting and deconvolution of the various spectral parameters were carried out using the GRAMS software.

3. Results and discussion

The molecular structures of compounds 7.O4O.7 and 7.O5O.7, their phase sequences and transition temperatures are shown in figure 1. The molecule can be broadly divided into three parts. There are two mesogenic groups, M and M′, connected by a flexible spacer, S. Earlier studies have considered the region MSM′ to be a semi-rigid core [1, 9]. Both 7.O4O.7 and 7.O5O.7 also contain terminal heptyl chains, (T and T′) which are attached to the two mesogenic segments M and M′.

As we are interested in investigating the effects of increasing the spacer length on the mesogenic region, we concentrated on spectral measurements in two

$H_{2m+1}C_m$-⬡-N=CH-⬡-O(CH$_2$)$_n$O-⬡-CH=N-⬡-C_mH_{2m+1}

|←—T—→|←—— M ——→|←— S —→|←—— M' ——→|←—T'—→|

$m = 7$
$n = 4$ for 7.O4O.7
$n = 5$ for 7.O5O.7

7.O4O.7: Cr ⟷ (115.5°C) SmF ⟷ (165.6°C) SmA ⟷ (212.8°C) I

7.O5O.7: Cr ——→ (108.5°C) SmA ⟷ (143°C) I
SmA ↓ (98.8°C) Sm F → (88°C) Cr

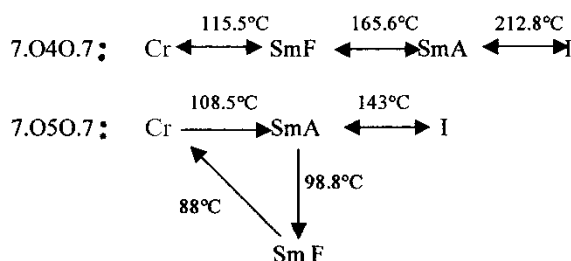Figure 1. General molecular structure of the liquid crystal dimers and the phase transition temperatures of compounds 7.O4O.7 and 7.O5O.7.

Table 1. Band assignments and dichroic ratios for the different Raman bands of 7.O4O.7 and 7.O5O.7.

7.O4O.7			7.O5O.7	
Band position cm^{-1}	Dichroic ratio	Band Assignment	Band position cm^{-1}	Dichroic ratio
1165	1.50	Aromatic C–H in-plane bending mode	1167	1.19
1172	1.61	C–O stretch	1172	1.37
1201	1.41	Aromatic C–N stretching mode	1195	1.17
		Quadrant stretching mode of the aromatic ring	1572	1.19
1577	1.87		1577	1.22
1595	1.63		1597	1.13
1602	1.21		1602	1.14
1627	1.40		1622	1.31

regions, namely, 1140–1220 and 1550–1650 cm^{-1} in which Raman bands arising from the functional groups of spacer and mesogenic units are expected. Another reason for selecting these spectral regions is the fact that the bands in these regions are comparatively strong and isolated. Bands in other regions, such as 2800–3200 cm^{-1} due to the alkyl chain modes, were extremely weak. In addition, as alkyl chains are present as both the spacer as well as terminal chains, only averaged information could be obtained from this region.
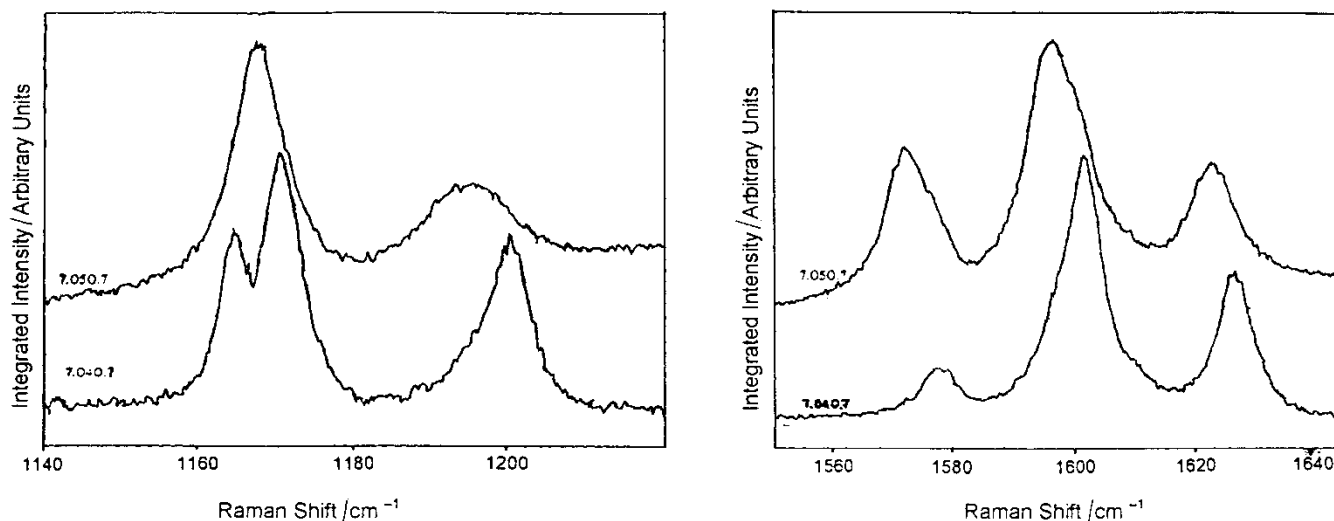
3.1. *Comparison of room temperature spectra of 7.O4O.7 and 7.O5O.7*

The 1140–1220 and 1550–1650 cm^{-1} regions of the Raman spectra of 7.O4O.7 and 7.O5O.7 at room temperature are shown in figures 2 (a) and 2 (b), respectively. The band assignments along with dichroic ratios (ratio of intensity of the bands with parallel and perpendicular polarizations) are shown in table 1. Peak positions, linewidths and integrated intensities for 7.O4O.7 and 7.O5O.7 in the crystalline state are given in table 2. The dichroic ratios for all the bands under study are greater than unity, suggesting some disorder in the individual segments of the molecules. Dramatic differences are observed between the room temperature spectra of 7.O4O.7 and 7.O5O.7, even though the only

Figure 2. Comparison of Raman spectra of 7.O4O.7 and 7.O5O.7 in the crystalline phase at room temperature.

Table 2.   The peak positions (cm^{-1}), linewidths (cm^{-1}) and integrated intensities of selected Raman bands for 7.O4O.7 and 7.O5O.7 at room temperature (crystalline phase). PP = peak position; LW = line width; II = integrated intensity.

	7.O4O.7			7.O5O.7	
PP	LW	II	PP	LW	II
1165	3.95	28.33	1167	7.05	50.64
1172	5.74	36.39	1172	3.91	14.40
1201	6.65	35.28	1195	11.73	34.94
—	—	—	1572	7.99	20.60
1577	6.85	9.28	1577	3.90	12.92
1595	7.41	11.43	1597	7.87	20.28
1601	7.08	49.96	1602	9.92	25.23
1627	7.01	29.33	1622	9.22	20.97

difference between the two compounds is an extra CH_2 group in the spacer region of 7.O5O.7. In the Raman spectra of 7.O4O.7, two distinct peaks appear at 1165 and 1172 cm^{-1} whereas in that of 7.O5O.7, one peak is clearly observed at 1167 cm^{-1} with an overlapping region at 1163 cm^{-1}. Differences are also observed in the 1570–1580 and 1590–1600 cm^{-1} regions of the spectra. The quadrant stretching modes related to the phenyl rings, which appear at 1595 and 1601 cm^{-1} for 7.O4O.7, show an upward shift of a few wave numbers and appear at 1597 and 1602 cm^{-1}, respectively, for 7.O5O.7. The band at 1577 cm^{-1} in the spectrum of 7.O4O.7, arising from the quadrant stretching mode of the benzene ring, splits into two in that of 7.O5O.7 with components at 1572 and 1577 cm^{-1}. The band at 1201 cm^{-1} due to the C–N stretching mode for 7.O4O.7 appears at 1195 cm^{-1}, showing a downward shift of 7 cm^{-1}, in the spectrum of 7.O5O.7. The band due to the C=N stretching mode shows a downward shift of 5 cm^{-1} from 1627 to 1622 cm^{-1} comparing the spectra of 7.O4O.7 and 7.O5O.7.

To understand these differences, we compare our results with some previously reported experimental results and theoretical calculations on similar types of dimeric liquid crystals [1, 9]. These studies have shown that the experimentally observed molecular length is less than the calculated all-*trans* molecular length. This has been explained by assuming a bent molecular shape deriving from the flexible spacer. Also the model assumes that the dimers exhibit different shapes depending on whether the spacers are odd or even, as shown in figure 3. Our observations using Raman spectroscopy support similar conclusions. The upward shifts of the peak positions for the phenyl ring-related modes indicate an increase in energy of the various bonds in 7.O5O.7, which suggests that, due to the change in shape (i.e. the increase in nonlinearity), the
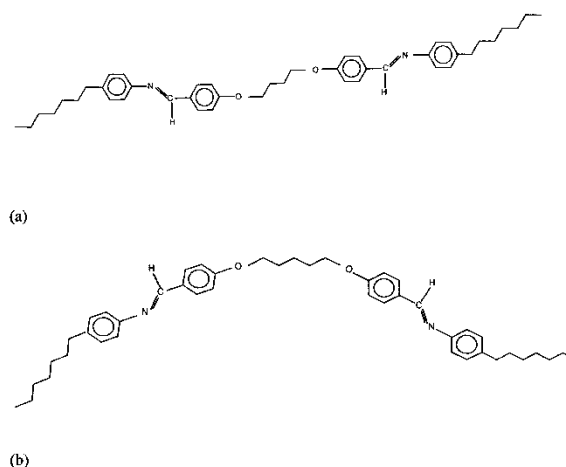

(a)

(b)

Figure 3.   Molecular shapes of (*a*) 7.O4O.7 and (*b*) 7.O5O.7.

7.O5O.7 molecule is capable of attaining an energetically favourable arrangement.

With regard to the C=N linkage mode, for 7.O4O.7 it appears at 1627 cm^{-1} which is the same position as that seen for the corresponding monomers, the *n*O.*m* series [16, 17]. It has been experimentally observed that the Schiff's base monomers of the *n*O.*m* and terephthalylidene-bis-*p*-*n*-alkylaniline (TBAA) series crystallize in a *c*–centered monoclinic lattice with a two-fold axis along the *b*- axis [18–20]. A visual comparison of the X-ray diffraction patterns of 7.O4O.7 and 7.O5O.7 with those of the monomers confirmed the existence of a monoclinic lattice for both 7.O4O.7 and 7.O5O.7. An X-ray powder photograph of 7.O5O.7 in the crystalline phase is shown in figure 4. A systematic analysis of the X-ray diffraction data of 7.O4O.7 and 7.O5O.7 in the crystal as well as the liquid crystal phases will be given in a future publication. It may be noted that in a recent single crystal X-ray diffraction study, the crystal structure of α-ω-bis(4-cyanobiphenyl-4′-yloxy)octane was established to be triclinic [21].

Figure 4.   X-ray powder photograph of 7.O5O.7 in the crystal phase.

Considering the bent structures of 7.O4O.7 and 7.O5O.7 in figure 3, we see that the structure of 7.O4O.7 is more or less identical to the structure of the monomeric compounds of the *n*O.*m* series, and it shows band positions in the Raman spectra similar to those of the monomers. In the case of the bow-like structure of 7.O5O.7, and also given the constraints of the monoclinic lattice, it is possible that either the different segments of the molecule twist along the single bonds or that there is distortion in some regions resulting in a weakening of the bonds. Twisting of the molecule along any of the single bonds such as C–O, Φ–O or Φ–N (Φ = phenyl ring) would have a greater impact on the bent shape. This is possible due to the constraints of the monoclinic lattice; the 7.O5O.7 molecules tend to attain a less bent shape and in doing so the C=N and C–N linkages are severely effected. In such cases the peak position of the band related to the mode is expected to be lowered. This is exactly what is observed in our studies in which the C=N stretching mode appears at 1622 instead of $1627\,cm^{-1}$.

We also see that the C=N linkage plays a greater role in determining the bent shape of the spacer. This is also supported by the changes that are observed in the linewidths and integrated intensities of the various bands. For the band related to the C–N linkage, a large change in linewidth is observed from 6.65 to $11.7\,cm^{-1}$ while the integrated intensity shows a small change. For the C=N stretching mode at $1627\,cm^{-1}$, the linewidth shows a small increase but a dramatic decrease is observed in the integrated intensity. This decrease in integrated intensity is accompanied by an increase of the integrated intensity for one of the C–H in-plane bending and one pair of quadrant stretching modes of the benzene ring. This clearly shows that there is a redistribution of the electron cloud from the C=N linkage towards one of the aromatic rings. This further substantiates our conclusion that the bent shape is affected by the C=N linkage. Therefore, in addition to the semi-rigid nature of the MSM′ core region, the C=N linkage plays a major role in the bent shape of the spacer.

3.2. *The crystal–smectic F transition*

Comparison of the Raman spectra of 7.O4O.7 and 7.O5O.7 in the crystalline, SmF and SmA phases are shown in figures 5 and 6, respectively. The peak positions, linewidths and integrated intensities of different bands in the crystal, SmF and SmA phases of 7.O4O.7 and 7.O5O.7 are given in tables 3 and 4 respectively. The crystal to smectic F (Cr–SmF) phase transition in 7.O4O.7 is accompanied by definite changes in all the spectral parameters of the system. These changes, i.e., in the peak positions, linewidths and integrated intensities, occur abruptly indicating the first order nature of this transition. The crystalline phase is characterized by a proper monoclinic lattice. The SmF phase, on the other hand, is characterized by a hexagonal clustering of the molecules with short range ordering. The major difference between these two phases is the hexagonal packing order of the molecules within the layered structure in the SmF and the crystalline structures.

The most significant spectral changes observed at the transition are the appearance of two bands at 1573
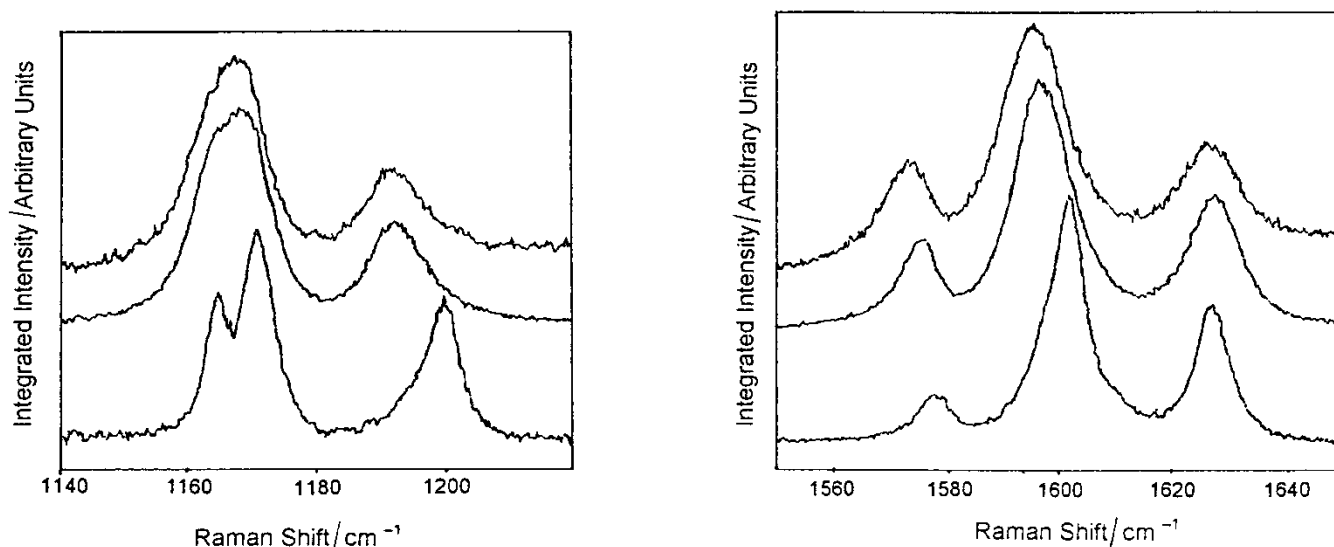

Figure 5. Comparison of the Raman spectra of 7.O4O.7 in the crystal, SmA and SmF phases.
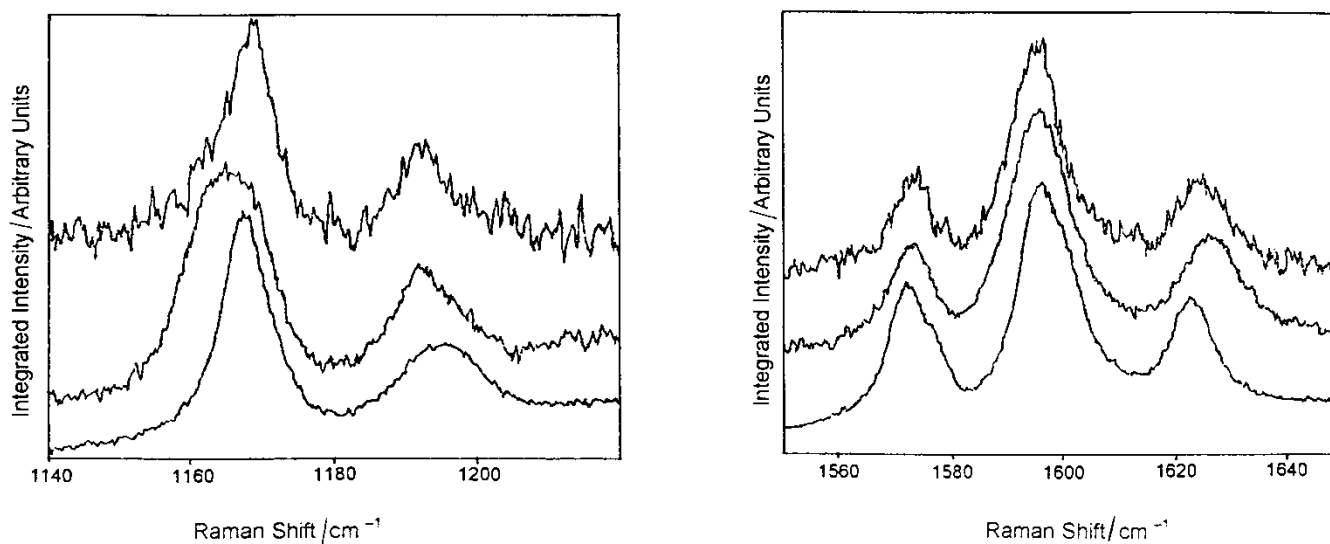
Figure 6. Comparison of the Raman spectra of 7.O5O.7 in the crystal, SmA and SmF phases.

Table 3. The peak positions (cm^{-1}), linewidths (cm^{-1}) and integrated intensities of selected Raman bands for 7.O4O.7 in the Crystal, SmF and SmA phases. PP = peak position; LW = line width; II = integrated intensity.

Crystal			SmF			SmA		
PP	LW	II	PP	LW	II	PP	LW	II
1165	3.95	28.33	1162	10.07	44.89	1163	8.7	36.75
1172	5.74	36.39	1166	6.71	28.31	1168	7.46	34.32
1201	6.65	35.29	1191	10.24	26.79	1193	10.24	28.93
—	—	—	1573	10.43	10.53	1576	8.56	7.54
1577	6.85	9.28	1576	5.76	6.19	1578	4.45	4.98
1595	7.41	11.43	1594	11.20	31.82	1596	9.31	30.36
1602	7.08	49.96	1598	10.57	28.00	1600	10.38	29.35
1627	7.01	29.33	1625	12.05	23.46	1627	10.27	27.28

Table 4. The peak positions (cm^{-1}), linewidths (cm^{-1}) and integrated intensities of selected Raman bands for 7.O5O.7 in the crystal, SmF and SmA phases. PP = peak position; LW = line width; II = integrated intensity.

Crystal			SmF			SmA		
PP	LW	II	PP	LW	II	PP	LW	II
1167	7.05	50.64	1163	9.22	25.31	1165	8.39	45.29
1172	3.91	14.40	1171	5.59	45.79	1172	6.45	28.21
1195	11.73	34.94	1192	7.65	28.89	1193	9.15	26.50
1572	7.99	20.60	1570	7.83	11.20	1569	7.09	9.30
1577	3.90	12.92	1575	4.07	5.15	1576	4.73	5.26
1597	7.87	20.28	1594	5.86	25.09	1595	9.48	28.29
1602	9.92	25.23	1598	10.15	35.00	1600	9.64	28.41
1622	9.22	20.97	1625	11.4	33.36	1627	11.05	28.74

and 1576 cm^{-1} in the SmF phase, in contrast to a single peak at 1577 cm^{-1} in the crystalline phase. Another major change observed in the SmF phase is a dramatic shift of the peak position of the C–N mode from 1201 in the crystalline phase to 1191 cm^{-1} in the SmF phase. The band associated with the C–O stretching mode at 1172 cm^{-1} also exhibits a shift towards lower wave numbers by 5 cm^{-1}; shifting from 1172 in the crystalline phase to 1166 cm^{-1} in the SmF phase. The C–H in-plane bending mode of the aromatic ring and the quadrant stretching modes show small changes in peak position towards lower wave numbers in the crystalline state, which now appears as an overlapping region in the SmF phase.

The changes in integrated intensity during this phase transition are also large. Generally, the line widths of almost all the bands show an increase, but the integrated intensities show quite irregular changes. The relative intensity of the band at 1162 cm^{-1} shows a major change when compared with the 1166 cm^{-1} band in the SmF phase. All these changes, when correlated, suggest that due to the relaxation of the lattice constraints of the crystalline phase and attainment of the layered structure, some deformations occur in the molecule along the C–N and C–O single bonds of the molecule. Also, the molecule can be considered to have a double mesogenic core; the short range ordering in the SmF phase results in rotation along the said single bond regions which, in turn, causes a change in the peak position of the C=N stretching band. The changes in the molecule suggest a shape that is more or less identical to that of the corresponding monomeric liquid crystals.

The crystal–SmF phase transition in 7.O5O.7 occurs on cooling the sample to 88°C from the monotropic SmF phase. In this case, the major changes in the peak positions are observed for the 1167 cm^{-1} phenyl

ring in-plane C–H stretching and the four quadrant stretching modes at 1572, 1577, 1597 and $1602 \, \text{cm}^{-1}$. For the C–N mode at $1195 \, \text{cm}^{-1}$, a downward shift is observed in the SmF phase in which it appears at $1192 \, \text{cm}^{-1}$. Simultaneously, the C=N stretching mode at $1622 \, \text{cm}^{-1}$ in the crystal phase appears at $1625 \, \text{cm}^{-1}$ in the SmF phase, exhibiting an upward shift of $3 \, \text{cm}^{-1}$ (table 4). By contrast the C–O stretching mode, shows only minimal changes. However, the changes in integrated intensities and linewidths are large for all the bands. All the changes observed for the crystal–SmF phase transition of 7.O5O.7 show that the semi-rigid bow-like shape is possible for this molecule, but there are still changes in the C=N linkage regions which tend to straighten the molecule.

3.3 *The SmF–SmA phase transition*

The SmF–SmA phase transition exhibited by 7.O4O.7 is accompanied by an abrupt change in peak positions, integrated intensities and linewidths of the different bands in the spectra indicating the first order nature of the transition. The SmF phase has a *c*–centered monoclinic lattice with strong in-plane short range positional correlations but almost negligible interlayer positional correlations. The molecules in this phase are tilted with respect to the layer planes and are packed in pseudo-hexagonal clusters. The SmA phase is characterized by a one-dimensional density wave whose wave vector is along the molecular director. It has a layered structure and maintains translational invariance within the smectic layer planes. The SmA phase is disordered and possesses only short range ordering between the molecules without the existence of any positional order.

The SmF–SmA phase transition is marked by changes in the peak positions of all the bands. As is clear from table 3, the peak positions of the Raman bands associated with the selected modes show a shift towards higher wave numbers by 2 to $3 \, \text{cm}^{-1}$, accompanied by changes in the linewidths and integrated intensities. The increase in the peak positions at the SmF–SmA transition is an indication of the increase in the freedom of the individual molecules in the clusters in the SmA phase. The changes in integrated intensities and linewidths point towards small changes in intermolecular positional/orientational ordering. Hence, we can conclude that the SmF–SmA transition in 7.O4O.7 is a manifestation of a transition between an ordered SmF phase to a disordered SmA phase. Also at this transition, it is observed that not only the individual segments, but the molecule as a whole is effected.

The only difference between 7.O4O.7 and 7.O5O.7 is an extra methylene unit in the spacer region of the molecule. This extra methylene unit has a profound effect on the molecular behaviour. Unlike 7.O4O.7, 7.O5O.7 exhibits a monotropic SmF phase with a lower transition temperature (only observed on cooling at 98.8°C) for the SmF–SmA phase transition. This phase transition in 7.O5O.7 is marked by the upward shift of peak positions by about $2 \, \text{cm}^{-1}$ when on moving from the SmF to the SmA phase. However, the position of the band due to the C–O mode remains unchanged at this transition. One of the quadrant-stretching modes of the aromatic ring at $1570 \, \text{cm}^{-1}$, however, shows a downward shift to $1569 \, \text{cm}^{-1}$.

The lower peak positions of the different modes in the SmF phase as compared with the SmA phase may be understood by considering the hexagonal clustering and short range ordering in the SmF phase. The changes in linewidths and integrated intensities are similar to those for 7.O4O.7, which again indicates small changes in the intermolecular orientational ordering. One major difference observed is that the C–O mode in 7.O5O.7 shows no change in position suggesting that in the SmF phase, due to hexagonal close clustering and the rigidity of the C–O portion, the bow-like structure of the molecule has become more curved. This increase of the bow-like structure of the molecule would result in the individual mesogenic parts behaving in a peculiar way. One can imagine that tilting the bow would result in one mesogenic segment being acutely tilted while the other mesogenic segment will be almost orthogonal due to the rigidity of the C–O region. This would lead to an unusual SmF phase, which is neither tilted nor orthogonal. This is exactly what has been found [1, 22] in X-ray diffraction studies in which the odd members exhibit unusual features in the diffraction patterns of the SmF phases.

Spectra in the isotropic phase could not be obtained in a reproducible fashion as the sample spread very thinly and became susceptible to laser heating and degradation.

References

[1] DATE, R. W., IMRIE, C. T., LUCKHURST, G. R., and SEDDON, J. M., 1992, *Liq. Cryst.*, **12,** 203.
[2] HEEKS, S. K., and LUCKHURST, G. R., 1993, *J. Chem. Soc., Faraday Trans.*, **89,** 3289.
[3] ATTARD, G. S., DATE, R. W., IMRIE, C. T., LUCKHURST, G. R., ROSKILLY, S. J., SEDDON, J. M., and TAYLOR, L., 1994, *Liq. Cryst.*, **16,** 529.
[4] DATE, R. W., LUCKHURST, G. R., SHUMAN, M., and SEDDON, J. M., 1995, *J. Physique II*, **5,** 587.
[5] FLETCHER, I. D., and LUCKHURST, G. R., 1995, *Liq. Cryst.*, **18,** 175.

[6] LE MASURIER, P. J., and LUCKHURST, G. R., 1998, *Liq. Cryst.*, **25,** 63.

[7] BLATCH, A. E., FLETCHER, I. D., LUCKHURST, G. R., 1997, *J. Mater. Chem.*, **7** BLATCH, A. E., and LUCKHURST G. R., 2000, *Liq. Cryst.*, **27,** 775.

[8] BARNES, P. J., DOUGLAS, A. G., HEEKS, S. K., and LUCKHURST, G. R., 1993, *Liq. Cryst.*, **13,** 603.

[9] FERRARINI, A., LUCKHURST, G. R., NORDIO, P. L., and ROSKILLY, S. J., 1993, *Chem. Phys. Lett.*, **214,** 3.

[10] ALAPATI, P. R., and LUCKHURST, G. R. unpublished results.

[11] GOGOI, B., ARULSANKAR, A., and ALAPATI, P. R., 2001, *Mol. Cryst. liq. Cryst.*, **366,** 69.

[12] GOGOI, B., ARULSANKAR, A., GHOSH, T. K., and ALAPATI, P. R., 2001, *Mol. Cryst. liq. Cryst.*, **365,** 561.

[13] FONTANA, M., and BINNI, S., 1976, *Phys. Rev. A.*, **14,** 1555.

[14] DASH, S. K., SINGH, R. K., ALAPATI, P. R., and VERMA, A. L., 1998, *Liq. Cryst.*, **25,** 459.

[15] DASH, S. K., SINGH, R. K., ALAPATI, P. R., and VERMA, A. L., 1999, *Liq. Cryst.*, **26,** 1479.

[16] BHATTACHARJEE, A., ALAPATI, P. R., and VERMA, A. L., 2001, *Liq. Cryst.*, **28,** 1315.

[17] BHATTACHARJEE, A., ALAPATI, P. R., and VERMA, A. L., 2002, *Liq. Cryst.*, **29,** 725.

[18] MORE, M., GORS, C., DEROLLEZ, P., and MATAVAR, J., 1995, *Liq. Cryst.*, **18,** 337.

[19] DOUCET, J., LEVELUT, A. M., and LAMBERT, M., 1974, *Phys. Rev. Lett.*, **32,** 301.

[20] BENETTAR, J. J., DOUCET, J., LAMBERT, M., and LEVELUT, A. M., 1979, *Phys. Rev. A.*, **20,** 2505.

[21] MALPEZZI, L., BRUCKNER, S., FERRO, D. R., and LUCKHURST, G. R., 2001, *Liq. Cryst.*, **28,** 357.

[22] GOGOI, B., and ALAPATI, P. R. unpublished results.